PHYSICAL REVIEW B VOLUME 38, NUMBER 7 1 SEPTEMBER 1988

Current oscillations in near-commensurate systems

A. R. Bishop
Theoretical Division and Center for Nonlinear Studies, Los Alamos National Laboratory, University of California, Los Alamos, New Mexico 87545

B. Horovitz*
Theoretical Division and Center for Nonlinear Studies, Los Alamos National Laboratory, University of California, Los Alamos, New Mexico 87545
and Laboratory of Atomic and Solid State Physics, Cornell University, Ithaca, New York 14853-2501

P. S. Lomdahl
Theoretical Division and Center for Nonlinear Studies, Los Alamos National Laboratory, University of California, Los Alamos, New Mexico 87545

(Received 1 February 1988)

The phenomena of current oscillations (CO) in response to a dc field is studied by the one-dimensional damped and field-driven sine-Gordon equation. For low damping we find that kink-antikink pairs survive collisions and CO through periodic boundaries is possible. For large damping CO is possible if the field is inhomogeneous, e.g., at contacts, creating kink-antikink pairs periodically. The results can account for data on charged-density waves and vortex lattice motion in superconducting films and annular Josephson junctions.

I. INTRODUCTION

A number of physical systems have shown in recent years that Josephson-type current oscillations exist in complex systems which cannot be reduced to a single degree of freedom. We define here the "current oscillation" (CO) phenomenon as generation of oscillation in time of an observable in response to a time independent field such that (a) the observable is averaged on all degrees of freedom and (b) the system cannot be reduced to that of an effective single degree of freedom. If (b) were not the case the system would obey a single pendulum type equation whose forced oscillations yield the conventional Josephson type effect, which we term as "commensurate current oscillation" (CCO).

The concept of commensurability is of center importance in our discussion below. When a periodic system slides relative to another periodic structure and the periodicities are commensurate (*C*), the motion may be reduced to that of a single center of mass coordinate in a periodic potential, resulting in CCO. If however the periodicities are incommensurate (IC) a single degree of freedom cannot describe the system and the less obvious CO phenomena may occur. Note that a *C* system may exhibit both CCO and CO phenomena.

The following systems are related to the CO phenomena: (a) Charge-density-wave (CDW) compounds such as $NbSe_3$, TaS_3, $K_{0.3}MoO_3$, $Rb_{0.3}MoO_3$, $(TaSe_4)_2I$ and $(NbSe_4)_{10}I_3$ which exhibit CO above a critical field.[1–6] The phenomena is termed here "narrow band noise;" the relation with "noise" is however misorienting since the generated oscillations have extremely well defined frequencies. The CDW wavelength is incommensurate (IC) but very close to being commensurate (*C*) with the underlying lattice, and in two cases [TaS_3, (Ref. 6) $K_{0.3}MoO_3$ (Ref. 7)] it becomes commensurate at lower temperatures. (b) A vortex lattice in a superconducting film whose thickness is modulated periodically in one direction.[8,9] The magnetic field controls the vortex periodicity which can be made *C* or IC relative to the periodicity of the thickness modulation. Oscillations were observed[8] in the *C* case and interpreted as a CCO.[10] The near-*C* situation however has also shown oscillations,[11] i.e., a CO phenomena. (c) An annular Josephson junction is an obvious candidate. The presence of fluxons in the junction corresponds to an IC situation and the usual Josephson effect vanishes when averaged along the junction. The possibility of oscillation even in this case[12,13] would correspond to a CO phenomena. (d) Growth oscillations[14] describe nonuniform cluster growth and a probability parameter defines an IC situation.

In the present work we model these systems by a one dimensional sine-Gordon equation with damping and a dc driving field and extend our previous study.[15,16] The model is presented in Sec. II together with several previously known results. Section III shows that kinks and antikinks survive collisions for *weak* damping. For a suitable initial condition CO persists by allowing the structure to repeat itself through the periodic boundaries. Section IV shows that in the *overdamped* case a nonuniform driving field can nucleate kink-antikink pairs periodically and lead to CO. In Sec. V we discuss experimental data and suggest that the CDW and vortex lattice data correspond to the case of Sec. IV, while annular Josephson junctions correspond to the case of Sec. III.

It is worth pointing out that we find CO in both *C* and IC situations for similar parameters. The CCO effect however is inherently a single-particle type phenomena; hence it cannot occur in incommensurate situations where space dependence, or the many degrees of freedom, are essential.

II. THE MODEL

Consider a classical one-space and time-dependent field $\psi(x,t)$ which satisfies

$$\ddot{\psi}(x,t)+\epsilon\dot{\psi}(x,t)-\psi''(x,t)+\sin\psi(x,t)=\Gamma \ . \qquad (1)$$

Here the overdot is $\partial/\partial t$, the prime is $\partial/\partial x$, ϵ is a damping parameter, and Γ is the dc driving field. Equation (1) is supplemented with $\mathrm{mod}(2\pi)$ periodic boundary conditions allowing for a density n_k of kinks in the length L

$$\int \psi'(x,t)dx/L=2\pi n_k \ . \qquad (2)$$

Each kink allows for a phase change of 2π. Thus, the C case has $n_k=0$ while $n_k\neq 0$ measures the deviation from commensurability. The observable current

$$\langle \dot{\psi} \rangle=\int dx\, \dot{\psi}(x,t)/L \qquad (3)$$

involves a crucial space average on all degrees of freedom. A significant property of (3) is that any traveling wave solution of the form $\psi(x-vt)$, though time dependent, does not produce CO—as seen from (2), $\langle \dot{\psi} \rangle=-2\pi v n_k$ is time dependent.

In the CDW case, $\psi(x,t)$ corresponds to the phase field of the order parameter.[17–19] A CDW with a commensurate wavelength Ma/N (with M,N reduced integers, a the lattice constant) has the form $\sim\cos(2\pi N x/Ma+\phi)$. This CDW can couple to the component of the lattice potential with periodicity a/N and produce an interaction energy $\sim\cos(M\phi)$; thus $\psi=M\phi$ in Eq. (1). In the IC case the CDW has the form

$$\sim\cos[(2\pi N/Ma+\delta q)x+\phi]$$

with the interaction energy $\sim\cos(M\phi+M\,\delta q\, x)$; thus, $\psi(x)=M\phi+M\,\delta q\, x$ and δq determines the boundary condition Eq. (2). Hence, n_k is a constant of the motion which is fixed by the total charge in the system. Furthermore, since the excess local charge is[19] $\sim\psi'(x,t)$ we have $\psi'(0,t)=\psi'(L,t)$ (the contacts do not sustain a difference in charge through the external circuit); i.e., periodic boundary conditions modulo $2\pi n_k L$.

For the vortex lattice $\psi(x,t)$ is a center of mass field,[9,20,21] the pinning force $\sim\sin\psi$ is due to the thickness modulation and Eq. (2) corresponds to deviation of the vortex average spacing from the period of the thickness modulation. For the annular junction $\psi(x,t)$ is the relative Josephson phase across the junction and (2) represents the net number of fluxons (i.e., fluxons minus antifluxons) in the junction.

Equation (1) with $n_k=0$ has single-particle type solutions, i.e., $\psi(x,t)=\psi(t)$ is space independent. This results in the well known CCO effect[22] above a threshold field which lies between $\Gamma_c(\epsilon=0)=0.725$ and $\Gamma_c(\epsilon>1.19)=1$.

The CO state, which is the main interest here, has a time dependent $\langle \dot{\psi} \rangle$ due to a nontraveling type $\psi(x,t)$. An important characteristic of a CO state is the ratio

$$\lambda=\langle\langle \dot{\psi} \rangle\rangle/\omega \qquad (4)$$

where $\langle\langle \dot{\psi} \rangle\rangle$ is the dc current (space and time average) and ω is the fundamental frequency of the CO. The meaning of λ follows from an effective single-particle coordinate $X(t)=a\langle \psi(x,t)\rangle/2\pi$; the 2π periodicity of ψ implies an underlying periodicity in X of length a. If the velocity $\dot{X}(t)$ is modulated with a period T due to an effective washboard potential with period a^* then $\langle \dot{X}(t)\rangle_t T=a^*$ where $\langle \ \rangle_t$ is a time average. Hence $\lambda=a^*/a$ measures an effective single-particle spatial periodicity.

A few properties of Eq. (1) with $n_k\neq 0$ were previously documented: When $n_k\neq 0$ and $\Gamma=0$ Eq. (1) can be easily integrated to show a static kink lattice with kink-kink spacing of $1/n_k$. When $\Gamma\neq 0$ Eq. (1) was shown[23] to have a traveling kink lattice solution of the form $\psi(x-vt)$. As shown above, this does not lead to CO.

Equation (1) can be solved analytically (Appendix) in two cases: (i) An expansion near the field $\Gamma_c=[1+(2\pi\epsilon n_k)^2]^{1/2}$ where the traveling wave has velocity $v=1$; (ii) A high velocity expansion which also yields a traveling wave solution. Neither case exhibits CO. In the next two sections we examine situations which result in a nontraveling wave solution with CO. In these numerical solutions we have mostly used a fourth-order spatial approximation of the second-order derivative, combined with a third-order Runge-Kutta method for the time integration. We also used a fast real-time simulation package[24] which generates movie like observations of the time evolution and allows for valuable intuition about the system.

III. UNDERDAMPED CASE

The sine-Gordon equation [$\epsilon=\Gamma=0$ in Eq. (1)] has well-known breather solutions.[25,26] Breathers are dynamic kink-antikink bound states which oscillate with frequency ω_B. Breathers can contribute to the current, Eq. (3), if the field can overcome their binding and produce free kinks and antikinks. Without damping ($\epsilon=0$) a threshold field for breakup $\Gamma(\omega_B)$ was found.[25] For lower ω_B the binding energy and $\Gamma(\omega_B)$ decrease so that $\Gamma(\omega_B)\to 0$ for $\omega_B\to 0$.

For $\epsilon\neq 0$ the lowest threshold Γ_c to unbind a $\omega_B\to 0$ breather is finite. To understand this qualitatively, consider a time t_0 when the oscillation passes through $\psi(x,t_0)=0$. To maintain the dynamics in Eq. (1) the field Γ must overcome the damping $\epsilon\dot{\psi}$; since $\dot{\psi}^2$ is of order of the kink-antikink energy $=16$ (at t_0 all the energy is kinetic) we obtain $\Gamma_c\sim\epsilon$. A more careful perturbation analysis[26] and numerical data[13] suggest $\Gamma_c\sim\epsilon^{0.8}$ for $\epsilon\lesssim 1$.

Figure 1 shows our results for the (Γ,ϵ) region where an initial breather with $\omega_B=0.2$ breaks up. The initial breather has a low-binding energy of ~ 0.3 and its threshold is close to that of the $\omega_B\to 0$ breather. We find that the C case is unstable at fields much *below* the single-particle threshold if ϵ is small. Once the breather is un-

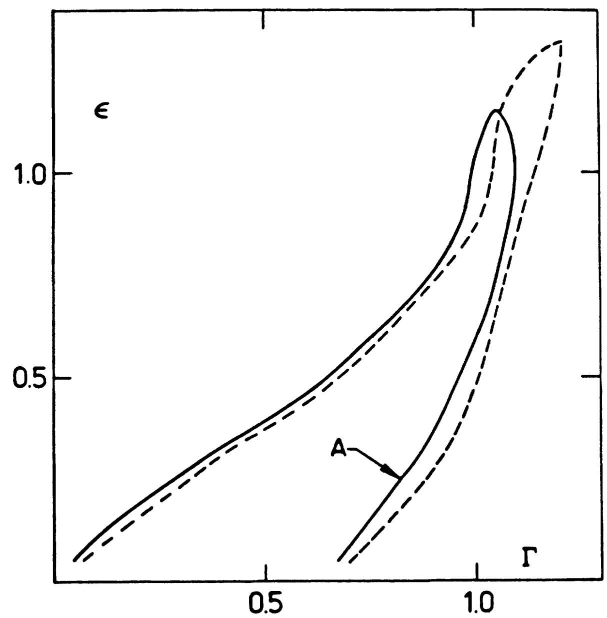

FIG. 1. Breather break-up regime yields CO for parameters inside the full line in a C case ($n_k=0$) or inside the dashed line in an IC case ($n_k=\frac{1}{24}$).

bound, the resulting kink-antikink pair travel around the ring and survive subsequent collisions. This nontrivial time dependence results in CO. Beyond the line A in Fig. 1 our initial breather leads to a traveling wave pattern with no CO. Depending on initial conditions,[16] a kink-antikink state can survive up to $\Gamma=1$, while for $\Gamma>1$ the single particle type CCO appear.

We have found that breather breakup persists even when $n_k\neq 0$ (dashed line in Fig. 1). Thus, the effect is more precisely a collision property i.e., the ability of kinks and antikinks to survive collisions. This property, which is well known in the undamped case, is a novel phenomena in a damped equation.

Figure 2 shows the time evolution of both C and IC cases. The collision property allows the pattern to periodically repeat itself after one revolution around the system. This results in CO as shown in Fig. 3 for a C case ($n_k=0$) and in Fig. 4 for an IC case ($n_k=\frac{1}{24}$).

Figure 5 shows current-field and ω-field dependence. There is a threshold field for the appearance of CO (as is

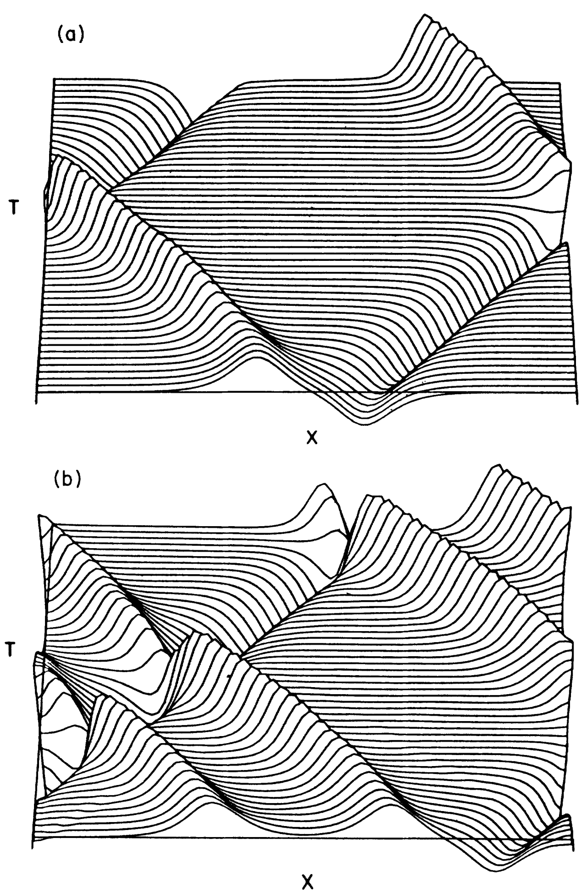

FIG. 2. Time evolution of $\psi'(x,t)$ showing that a kink (peak) passes through an antikink (dip). Time runs upward for approximately 23 unit, $0\leq x\leq 24$, $\epsilon=0.3$, and $\Gamma=0.5$. (a) C case (b) IC case, $n_k=\frac{1}{24}$.

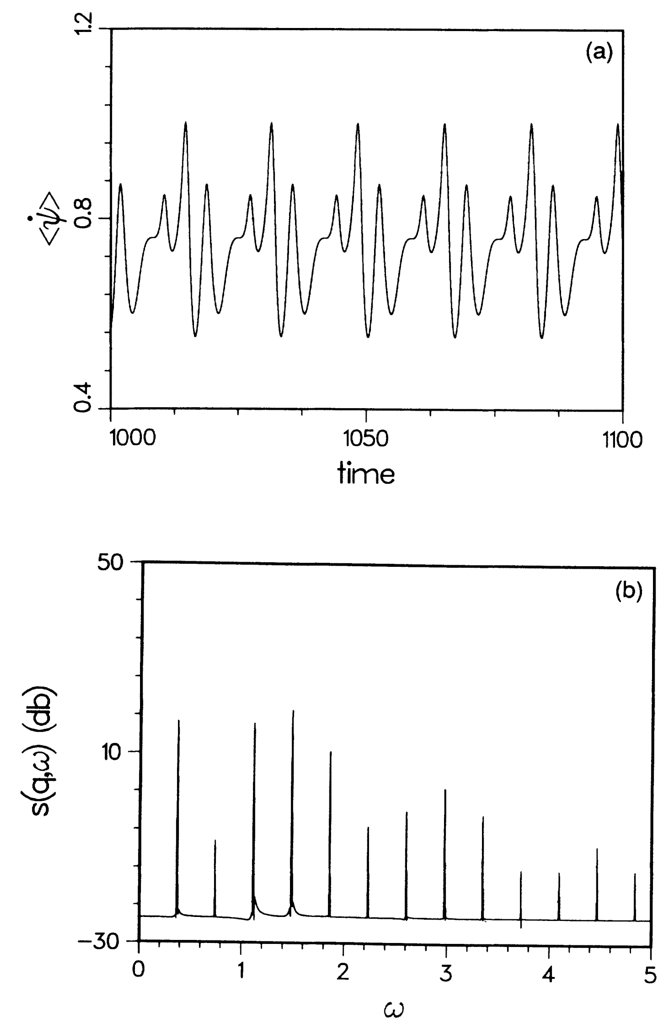

FIG. 3. (a) Time dependence of $\langle\dot{\psi}\rangle$ for $\epsilon=0.3$, $\Gamma=0.5, n_k=0$, and a single kink-antikink pair. (b) power spectrum of (a).

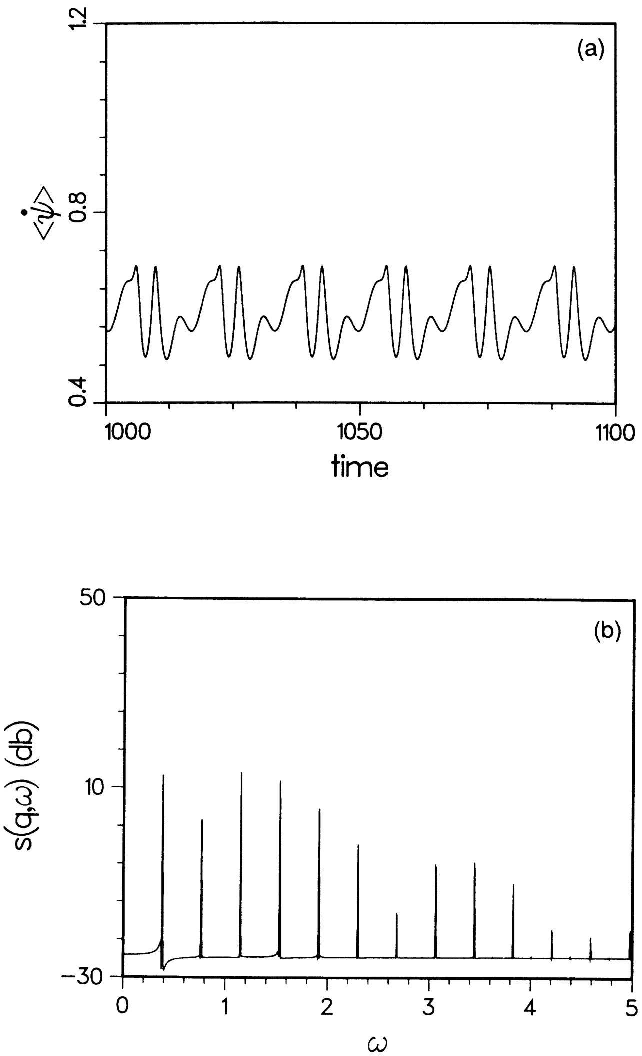

FIG. 4. (a) Time dependence of $\langle \dot{\psi} \rangle$ for $\epsilon=0.3$, $\Gamma=0.5$, $n_k=\frac{1}{24}$, and an additional kink-antikink pair. (b) Power spectrum of (a).

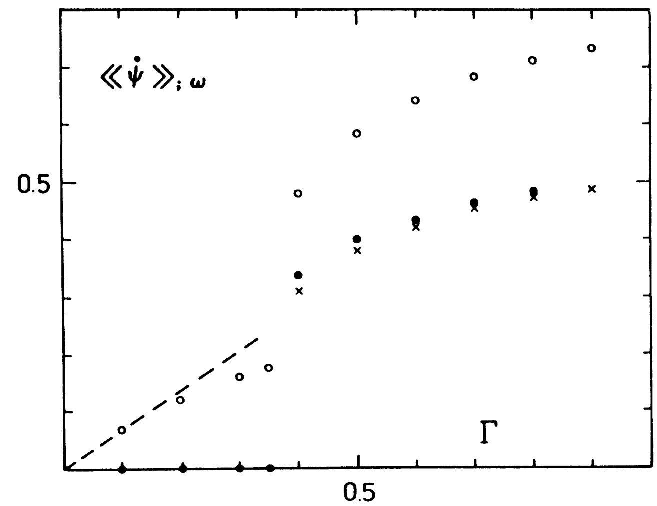

FIG. 5. The dc current $\langle\langle \dot{\psi} \rangle\rangle$ (○) and the CO frequency ω (×) for an IC case $n_k=\frac{1}{24}$ and $\epsilon=0.3$. For the C case $\langle\langle \dot{\psi} \rangle\rangle=\omega$ is shown by dots. The dashed line is the ohmic linear response of a kink (e.g., Ref. 22).

evident from Fig. 1) for both C and IC cases. Note that $\langle\langle \dot{\psi} \rangle\rangle$ is finite in the IC case below this threshold due to a traveling wave solution.

To estimate λ [Eq. (4)] consider N_k kinks and N_B kink antikink pairs, the latter generated, e.g., from N_B breathers. After one revolution around the length L in time T the phase increase $2\pi(2N_B+N_k)$ should equal $\langle\langle \dot{\psi} \rangle\rangle T$. Since the space inverted structure is equivalent to the original one we expect $\omega=4\pi/T$, hence $\lambda=N_B+\frac{1}{2}N_k$.

We have found that numerical values of λ are indeed close to $N_B+\frac{1}{2}N_k$, as shown in Table I. We find that λ is independent of ϵ or Γ except for small changes near the boundaries in Fig. 1. Note also that the dc and ac currents are intensive quantities which depend mainly on the densities N_k/L, N_B/L. The frequency ω and the ratio λ, however, depend on L so that this CO phenomena is a finite-size effect. This is quite different from CCO for which $\lambda=1$ is independent of L.

TABLE I. CO data for $\epsilon=0.5$, $\Gamma=0.8$ for various numbers of breathers (or kink-antikink pairs) N_B, kinks N_K and chain lengths L. CO frequency is ω, dc current is $\langle\langle \dot{\psi} \rangle\rangle$, amplitude of ac current is $\langle \dot{\psi} \rangle_{ac}$ and $\lambda=\langle\langle \dot{\psi} \rangle\rangle/\omega$.

N_K	N_B	L	$\langle\langle \dot{\psi} \rangle\rangle$	$\langle \dot{\psi} \rangle_{ac}$	ω	λ
0	1	12	0.766	0.50	0.763	1.00
0	1	24	0.404	0.23	0.403	1.00
0	2	24	0.740	0.50	0.368	2.01
0	2	48	0.404	0.22	0.203	1.99
1	1	12	1.101	0.48	0.698	1.58
1	1	18	0.759	0.30	0.494	1.54
1	1	24	0.585	0.22	0.382	1.53
1	1	48	0.309	0.11	0.205	1.51
1	2	24	0.903	0.50	0.351	2.56
1	2	48	0.494	0.23	0.196	2.53
2	2	48	0.585	0.22	0.192	3.05

IV. OVERDAMPED CASE

Data on the CDW (Ref. 2 and 3) and vortex lattice[8,9] systems indicate an overdamped situation, $\epsilon \gg 1$. As we now show, CO is present for $\epsilon \gg 1$ if the dc field Γ is nonuniform in space. This corresponds to the role of contacts in the CDW case, where we expect a stronger field than in the bulk. Also in the case of a superconducting film, it is known that the current (which is the driving force for the vortex motion) is higher at the film edges.[27]

We consider Γ in (1) of the form

$$\Gamma = \Gamma_0 + A\,\delta(x)\ . \tag{5}$$

In the C case a static solution (with periodic boundaries) is possible by matching kink and antikink tails at $x=0$ so that the discontinuity in the slope is A. Since the maximal slope of a kink $[\psi(x)=4\tan^{-1}[\exp(x)]$ is 2, a static solution is not possible for $A>4$. Thus, for $A<4$ we expect a finite threshold field Γ_0 for generating a dynamic solution. (The lattice discreteness in the numerical simulation in fact allows a slightly higher critical A.) In the IC case a static solution as above is not possible and all $\Gamma_0 \neq 0$ should generate a dynamic solution.

As shown in Fig. 6 the effect of the localized field $A\,\delta(x)$ is to generate periodically a kink-antikink pair. Since $\epsilon \gg 1$ these kinks annihilate away from $x=0$ after collisions. The corresponding CO is shown in Figs. 7–9 for $A=4.17$ where the threshold field is very low, $\Gamma_0 \simeq 0.01$. We use $\epsilon=10$ for all data in this section, as a representative $\epsilon \gg 1$ case.

Figure 7 shows a C case near threshold ($\Gamma_0=0.02$). Each period has two peaks corresponding to the two events of nucleation and annihilation. This results in a rich harmonic content, with the intensity of the nth harmonic decaying nonmonotonically. Figure 8 shows the C case with a stronger field $\Gamma_0=0.2$. The component of the time-dependent part in $\langle \dot{\psi} \rangle$ is now smaller, the harmonic content is however, still significant with the nth harmonic intensity decaying exponentially as $\sim (0.0076)^n$.

Figure 9 shows the effect of the kink density on CO. Although the amplitude of the time-dependent part is somewhat reduced, it is quiet remarkable that $n_k = \frac{5}{24}$ has a significant CO. The effect of the periodic potential on the space modulation is very weak [see Fig. 9(c)], yet the dynamic effect in the *time* modulation is still significant.

Figure 10 shows a case with $A=3.0$ and $\Gamma_0=4.0$, for which the threshold is $\Gamma_0 \simeq 0.3$. An increase in n_k again has a weak effect on the CO strength, though a stronger effect on reducing the harmonic content.

To evaluate the λ ratio [Eq. (4)], consider $x=0$ where

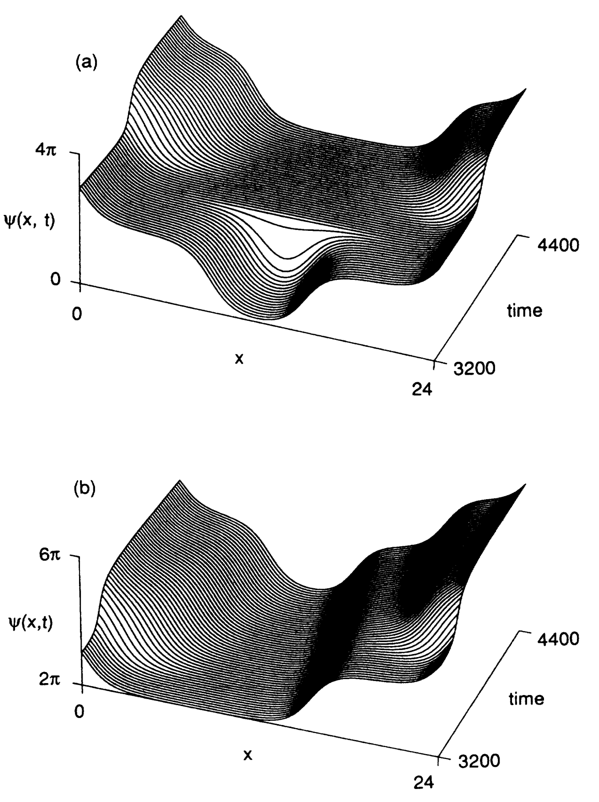

FIG. 6. Time evolution of $\psi(x,t)$ with inhomogeneous field $\Gamma_0=0.02$, $A=4.17$ [Eq. (5)], $\epsilon=10$, and (a) $n_k=0$, (b) $n_k=\frac{1}{24}$.

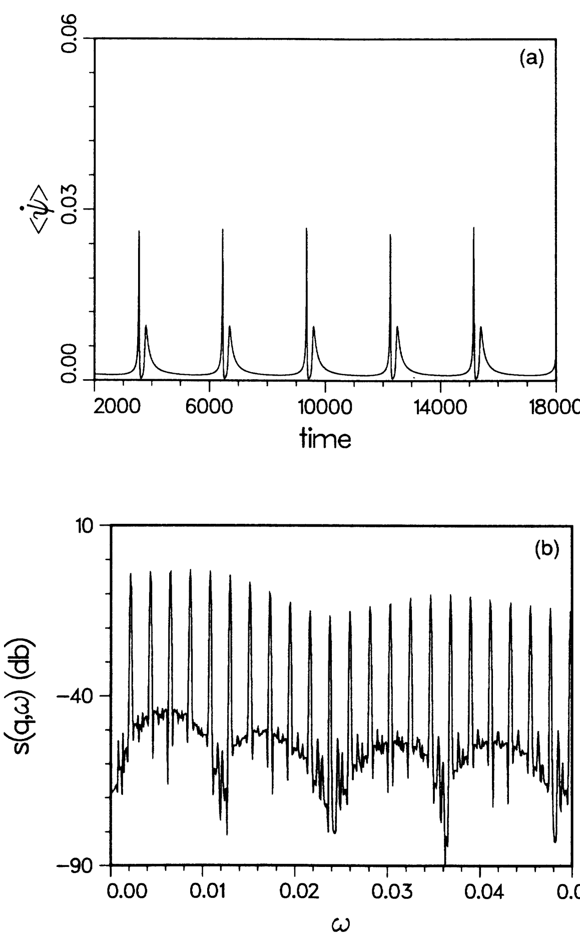

FIG. 7. (a) Time dependence of $\langle \dot{\psi} \rangle$ for $\Gamma_0=0.02$, $A=4.17$, $\epsilon=10$, and $n_k=0$. (b) Power spectrum of (a).

CO originate. If the nucleation rate is one pair in time T then the phase change is $\langle \dot{\psi}(x=0,t) \rangle_t T = 2\pi$. For long times t the phase $\psi(x=0,t)$ can differ by only a finite amount from $\psi(x\neq 0,t)$ so that $\langle \dot{\psi}(x=0,t) \rangle_t$ can be replaced by a time *and* space average, i.e., $\langle \langle \dot{\psi}(x,t) \rangle \rangle T = 2\pi$. Hence, $\lambda = 1$ [Eq. (4)] and the system appears as if it were commensurate with CCO.

We have confirmed numerically that indeed $\lambda=1$. Figure 11 shows the fundamental frequency ω (which equals $\langle \langle \dot{\psi} \rangle \rangle$) as function of Γ_0 for a few cases. As previously discussed, the $n_k=0$ cases have a finite threshold in Γ_0 while the $n_k \neq 0$ cases have no threshold.

V. DISCUSSION

The CO phenomena has been extensively studied in CDW systems. The theoretical description of CO, or "narrow band noise" has so far been of two types. A contact approach considers generation of vortices[28,29] or phase slip centers[30] at the boundary between a moving CDW and a CDW at rest. The vortex model shows the formation of two-dimensional defects, but does not account for the coherence of their generation at a rough contact. The phase slip model shows in a one-dimensional model that a smooth effective boundary can appear even if the contact itself is rough. Though controversial[2,4] there is in fact considerable experimental support for CO being generated at the contacts.[29] The second approach considers impurity pinning which forms finite domains.[2,31] While impurities affect the threshold field and the nonohmic response, it is not obvious that many domains will act coherently to produce CO; in fact the vortex lattice system (see the following) indicates that they do not.

In our approach, once the CDW is depinned from impurities, CO is generated by its interaction with the

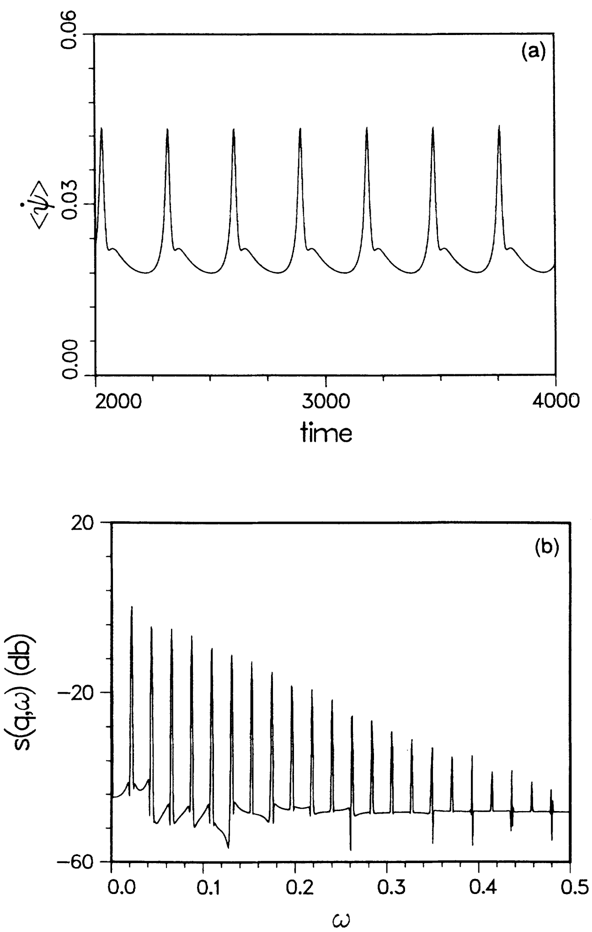

FIG. 8. Same as Fig. 7 except $\Gamma_0=0.2$.

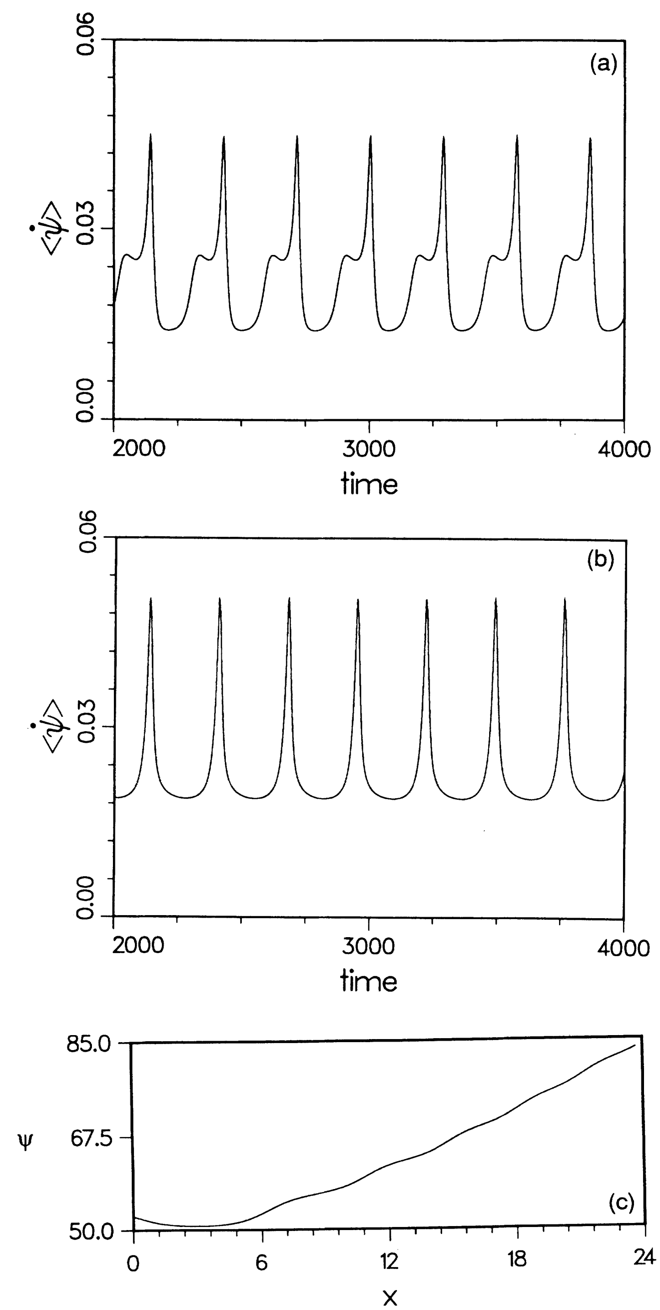

FIG. 9. Effect of n_k on time dependence of $\langle \dot{\psi} \rangle$ for $\Gamma_0=0.2$, $A=4.17$, $\epsilon=10$: (a) $n_k=\frac{1}{24}$, (b) $n_k=\frac{5}{24}$. The space dependence of $\psi(x,t)$ for case (b) at $t=4000$ is shown in (c).

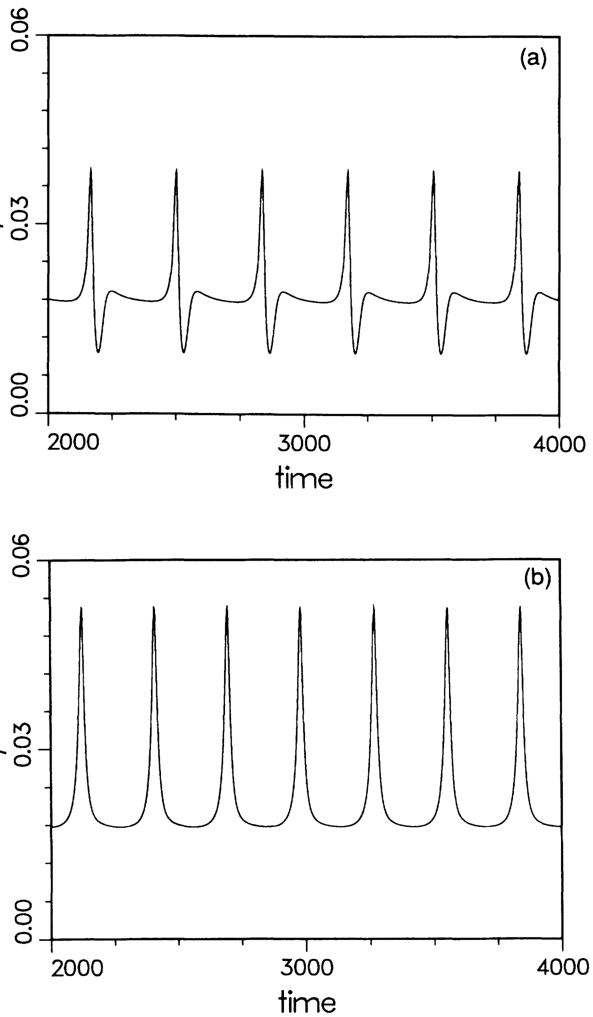

FIG. 10. Time dependence of $\langle \dot{\psi} \rangle$ for a weaker "contact" field, i.e., $\Gamma_0=0.4$, $A=3.0$, $\epsilon=10$: (a) $n_k=0$, (b) $n_k=\frac{2}{24}$.

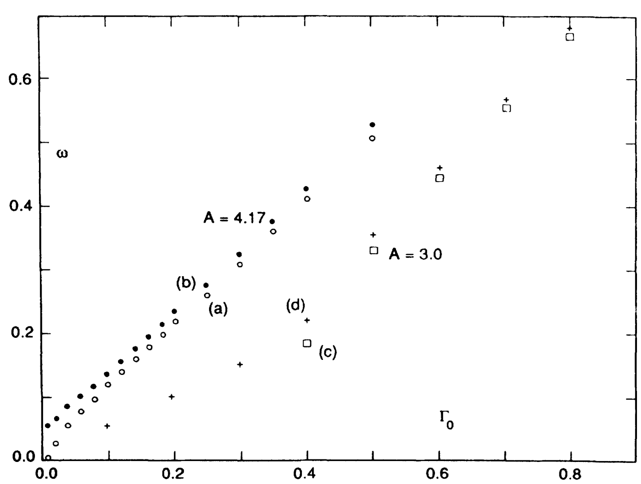

FIG. 11. The dc current $\langle\langle \dot{\psi} \rangle\rangle$ (or CO frequency $\omega=\langle\langle \dot{\psi} \rangle\rangle$) as function of field Γ_0 for $\epsilon=10$ and (a) $A=4.17$, $n_k=0$ (○); (b) $A=4.17$, $n_k=\frac{5}{24}$ (●); (c) $A=3.0$, $n_k=0$ (□); (d) $A=3.0$, $n_k=\frac{2}{24}$ (×).

periodic lattice potential. In particular in the two cases (TaS_3 in Ref. 6, $K_{0.3}MoO_3$ in Ref. 7) which become *commensurate* at lower temperature, the lattice periodicity must be relevant. However, estimates of the threshold field[6,32] for CCO [$\Gamma=1$ in the units of Eq. (1)] yield values much higher than the experimental ones. Furthermore, the threshold field, the CO frequencies and intensities are similar in both C and IC cases.

Since the CDW systems are overdamped[2,3] ($\epsilon \gg 1$) we apply the results of Sec. IV to resolve the above difficulties. The commensurability potential is indeed relevant in both C and IC cases, yet CO can appear at $\Gamma \ll 1$ if the field is inhomogeneous [curves (a) and (b) in Fig. 11]. The observation of significant harmonic content even at high fields[4] is consistent with our results (see e.g., Fig. 8). The change in harmonic content from one scan to another[5] may be due to a change in the field profile near the contacts.

The static solution to Eqs. (1) and (2) ($\Gamma=0$) is a kink lattice which generates harmonic satellites in x-ray scattering. However, only a weak second harmonic was seen in $NbSe_3$.[33] This harmonic content depends on the product $n_k\xi$, where ξ is the single kink width [$\xi=1$ in the units of Eq. (1)]. Evaluation of the ac conductivity (i.e., linear response to an oscillating field) of a kink lattice has shown[34] that $n_k\xi \simeq 0.2$ is consistent with the data. For $n_k\xi \gtrsim 0.2$ [Fig. 9(c)] the structure factor contains weak harmonics and we might expect that the commensurability potential is irrelevant. This, however, is not the case since the dynamic harmonic content is much more pronounced than the static one. This is demonstrated in Figs. 9(b) and 9(c) where very weak spatial modulations of the phase yield surprisingly strong modulations in time, representing CO.

Another reason for smoothing the spatial structure are long range Coulomb interactions[35] [not included in Eq. (1)]; this may correspond to effectively increasing ξ. We also expect that Coulomb interactions in the contact area are more effectively screened and the effects of commensurability can be more pronounced. This will enhance the dynamic harmonic content of the nucleation process which probably occurs predominantly in the contact area.

The periodicity length $a^*=\lambda a$ can be estimated experimentally if the effective CDW charge ne moving at velocity v is known. The current $J=nev$ and frequency $\omega=2\pi v/a^*$ yield $J/\omega=nea^*/2\pi$. The data[36] suggests $\lambda \simeq 2$ which differs from our result $\lambda=1$, but also differs from other theories[2,28-31] where a^* is the CDW wavelength and $\lambda \simeq 4$. With the uncertainty in the CDW charge (ne) it seems that at present the λ ratio cannot determine which theory is consistent. Fortunately this uncertainty is avoided in the vortex lattice system which we next discuss.

The dynamics of a vortex lattice in a superconducting film provide an ideal arrangement for a direct comparison of experiment with theory.[8-10] One can directly control the commensurability potential and the deviation from commensurability (n_k), and even measure the λ ratio. Consider first a flat film where the only potentials are due to random impurities. The data show that mode locking is present,[37] i.e., an external ac field can phase lock the various domains and lead to steps in the I–V curves. The CO phenomena, however, seems to be absent.[37] Thus, in a dc voltage the current oscillations of various domains add incoherently and an ac response is not generated.

Effects of commensurability can be demonstrated by periodically modulating the film thickness in one direction, as shown by Martinoli *et al.*[8] A magnetic field B_z in the z direction which moves in the x direction generates an electric field $E_y = vB_z/c$ so that the velocity v can be directly determined. If a is a periodicity of the thickness modulation (in the x direction) then the frequency

$$\omega = 2\pi v/a = 2\pi c E_y / B_z a \tag{6}$$

is expected. Equation (6) corresponds to $\lambda = 1$ in Eq. (4). By changing B_z the periodicity of the vortex lattice is changed, i.e., the commensurability parameter n_k is easily controlled.

The data[8] shows that at commensurability ($B_z = B_m$) current oscillations appear and Eq. (6) is satisfied. For small deviations from B_m the vortex lattice can deform and still be pinned by the thickness modulation[8,9] and current oscillations persist with ω fixed at the B_m value of Eq. (6). This scenario has been interpreted as CCO, i.e., a single-particle type oscillation.[8] Further data, however, shows[8,11] that even for larger $B_z - B_m$, where the vortex lattice is IC, the oscillations persist and that Eq. (6) is obeyed.

It is known that the current distribution in a thin superconducting film in a magnetic field is peaked near the film edges.[27] Since the current is the driving force[20] Γ in Eq. (1) we are justified in using the inhomogeneous field model of Sec. IV. We therefore suggest that the observed oscillation in vortex lattice motion in both C and IC cases is a CO phenomena which occurs due to kink-antikink nucleation at the film boundaries.

The third system which is relevant is an annular Josephson junction. Since this is an underdamped system the scenario of Sec. III is relevant. Experiments in this system show that a variety of kink and antikink combinations is feasible.[12,13] We propose that observation of CO is an additional useful tool of probing the various states.

In conclusion we have shown two types of CO phenomena. The first type occurs in an underdamped system due to the capability of kinks and antikinks to survive collisions. The second type occurs even in overdamped systems and is due to space inhomogeneity of the driving force.

ACKNOWLEDGMENTS

We thank P. Martinoli for stimulating discussions. This research was supported by a grant from the U.S.-Israel Binational Science Foundation (Jerusalem, Israel).

APPENDIX

We present here analytic results for Eq. (1) with a uniform field Γ for two cases: (i) a moving kink lattice with velocity near $v = 1$, (ii) a high velocity expansion. A solution of the form $\psi(x+vt)$ with $v = 1$ satisfies $\ddot{\psi}(x+t) = \psi''(x+t)$, hence, Eq. (1) implies

$$\epsilon\dot{\psi}(x+t) + \sin[\psi(x+t)] = \Gamma\ . \tag{A1}$$

Equation (A1) by itself has a critical field $\Gamma = 1$ so that for $\Gamma < 1$ $\psi = \sin^{-1}(\Gamma)$ and $\langle\langle\dot{\psi}\rangle\rangle = 0$ while for $\Gamma > 1$

$$\dot{\psi}(x+t) = (\Gamma\epsilon)^{-1}(\Gamma^2 - 1)/\{1 + \Gamma^{-1}\sin[(x+t)(\Gamma^2-1)^{1/2}/\epsilon]\}\ . \tag{A2}$$

Equation (A2) yields the current-field relation

$$\langle\langle\dot{\psi}\rangle\rangle = (\Gamma^2 - 1)^{1/2}/\epsilon\ . \tag{A3}$$

The solution (A2) is however relevant only if it satisfies the boundary condition (2), which implies $\langle\langle\dot{\psi}\rangle\rangle = \langle\psi'\rangle = 2\pi n_k$. This is consistent with (A3) only if $\Gamma = \Gamma_c$ where

$$\Gamma_c = [1 + (2\pi n_k \epsilon)^2]^{1/2}\ . \tag{A4}$$

Hence, Eq. (A2) is a valid solution $\psi_c(x,t)$ only at $\Gamma = \Gamma_c$.

The solution near Γ_c can be found by expanding around $\psi_0(x,t)$ where

$$\dot{\psi}_0(x,t) = (\Gamma\epsilon)^{-1}(\Gamma^2-1)/\{1 + \Gamma^{-1}\sin[x(\Gamma_c^2-1)^{1/2}/\epsilon + t(\Gamma^2-1)^{1/2}/\epsilon]\}\ . \tag{A5}$$

Note that $\psi_0(x,t)$ has the same space periodicity as $\psi_c(x,t)$ so that (2) is satisfied. The time periodicity of (A5), however, is different from that of $\psi_c(x,t)$ so that $\psi_0(x,t)$ satisfies (A1) and secular terms in t are not generated. A solution $\psi(x,t) = \psi_0(x,t) + \chi(x,t)$ with $\chi = O(\Gamma - \Gamma_c)$ can be found by expansion in χ. Using $\chi'' - \ddot{\chi} = O(\Gamma - \Gamma_c)^2)$ we find, up to a rigid t translation of ψ_0,

$$\chi(x,t) = (\Gamma_c^2 - \Gamma^2)/[\epsilon(\Gamma^2-1)]\dot{\psi}_0(x,t)\ln\dot{\psi}_0(x,t)\ . \tag{A6}$$

Since $\chi(x,t)$ is periodic, $\langle\langle\dot{\chi}\rangle\rangle = 0$ and the current-field relation is given by (A3); thus, (A3) is exact near $\Gamma = \Gamma_c$ to order $\Gamma - \Gamma_c$.

The second case considered here is a high velocity expansion. For $\Gamma \to \infty$ the solution of Eqs. (1) and (2) is

$$\psi(x,t) = \Gamma t/\epsilon + 2\pi n_k x\ . \tag{A7}$$

To find $O(1/\Gamma)$ terms consider

$$\psi(x,t)=vt+2\pi n_k x+\tilde{\psi}(x,t) \tag{A8}$$

and v is determined below to avoid secular terms in t. Equation (1) reduces to an integral equation for $\tilde{\psi}(x,t)$

$$\tilde{\psi}(x,t)=\int dx'dt' \sum_{k,w} e^{ik(x-x')-i\omega(t-t')}G(k,\omega)\{\Gamma-v\epsilon-\sin[vt'+2\pi n_k x'+\tilde{\psi}(x',t')]\} , \tag{A9}$$

where

$$G(k,\omega)=[-\omega^2+k^2-i\omega\epsilon]^{-1} . \tag{A10}$$

The $\Gamma-v\epsilon$ term in (A9) yields

$$\tilde{\psi}_0(x,t)=(\Gamma/\epsilon-v)t . \tag{A11}$$

This secular term will be canceled below. The lowest order term of $\tilde{\psi}$ is obtained by setting $\tilde{\psi}=0$ on the right-hand side of (A9),

$$\tilde{\psi}_1(x,t)=\tfrac{1}{2}ie^{ivt+2\pi i n_k x}G(2\pi n_k,-v)+\text{H.c.} \tag{A12}$$

The final order considered here is obtained by expanding the right hand side of (A9) with $\tilde{\psi}=\tilde{\psi}_1$,

$$\tilde{\psi}_2(x,t)=-iG(2\pi n_k,-v)[t/\epsilon+G(4\pi n_k,-2v)e^{2i(2\pi n_k x+vt)}]/4 . \tag{A13}$$

To cancel the diverging term linear in t we choose

$$v=(\Gamma/\epsilon)\{1-[2(\Gamma^2/\epsilon^2-4\pi^2 n_k^2)^2+2\Gamma^2]^{-1}\} . \tag{A14}$$

With this choice $\tilde{\psi}(x,t)=0(1/\Gamma)$ is periodic and (A8) yields $\langle\langle\dot{\psi}\rangle\rangle=v$; thus the current-field relation approaches the curve (A3) from above.

We note that in both cases considered in this appendix the solutions are traveling waves and do not exhibit CO. The regions of Γ near $\Gamma_c>1$ and $\Gamma\gg 1$ are indeed out of the CO regime of Fig. 1.

*On leave from the Department of Physics, Ben-Gurion University, 84 105 Beer-Sheva, Israel.

[1]R. M. Fleming and C. C. Grimes, Phys. Rev. Lett. **42**, 1423 (1979); R. M. Fleming, Phys. Rev. B **22**, 5506 (1980).
[2]For a review see G. Gruner and A. Zettl, Phys. Rep. **119**, 117 (1985).
[3]For a review see P. Monceau, in *Electronic Properties of Inorganic Quasi One Dimensional Materials,* edited by P. Monceau (Reidel, New York, 1985), Vol. 2, p. 139.
[4]R. E. Thorne, W. G. Lyons, J. W. Lyding, J. R. Tucker, and J. Bardeen, Phys. Rev. B **35**, 6348 (1987); **35**, 6360 (1987).
[5]S. Bhattacharya, J. P. Stokes, M. J. Higgins, and R. A. Klemm, Phys. Rev. Lett. **59**, 1849 (1987).
[6]Z. Z. Wang, H. Salva, P. Monceau, J. Richard, C. Roucau, R. Ayrolles, F. Levy, L. Guemas, and A. Meerschaut, J. Phys. (Paris) Lett. **44**, L311 (1983).
[7]J. P. Pouget, S. Kagoshima, C. Schlenker, and J. Marcus, J. Phys. (Paris) Lett. **44**, L113 (1983).
[8]P. Martinoli, O. Daldini, C. Leeman, and B. Van Den Brandt, Phys. Rev. Lett. **36**, 382 (1976).
[9]P. Martinoli, O. Daldini, C. Leeman, and E. Stocker, Solid State Commun. **17**, 205 (1975).
[10]P. Martinoli, Phys. Rev. B **17**, 1175 (1978).
[11]P. Martinolli, private communication.
[12]A. Davidson and N. F. Pederson, Appl. Phys. Lett. **44**, 465 (1984).
[13]A. Davidson, B. Dueholm, B. Kryger, and N. F. Pedersen, Phys. Rev. Lett. **55**, 2059 (1985).
[14]Z. Cheng, R. Baiod and R. Savit, Phys. Rev. A **35**, 313 (1987).
[15]B. Horovitz, A. R. Bishop, and P. S. Lomdahl, Physica B **143**, 135 (1986).
[16]J. C. Ariyasu and A. R. Bishop, Phys. Rev. B **35**, 3207 (1987).
[17]S. N. Artemenko and A. F. Volkov, Zh. Eksp. Teor. Fiz. **81**, 1872 (1981) [Sov. Phys.—JETP **54**, 992 (1981)].
[18]B. Horovitz and J. A. Krumhansl, Phys. Rev. B **29**, 2109 (1984).
[19]For a review see B. Horovitz in *Solitons,* edited by S. E. Trullinger, V. E. Zakharov, and V. L. Pokrovski (North-Holland, Amsterdam, 1986), p. 691.
[20]A. Schmid and W. Hauger, J. Low Temp. Phys. **11**, 667 (1973).
[21]S. E. Burkov and V. L. Pokrovskii, J. Low Temp. Phys. **44**, 423 (1981).
[22]W. C. Stewart, Appl. Phys. Lett. **12**, 277 (1968); D. E. McCumber, J. Appl. Phys. **39**, 3113 (1968).
[23]P. M. Marcus and Y. Imry, Solid State Commun. **33**, 345 (1980).
[24]P. S. Lomdahl (unpublished). The real-time simulation package which runs on SUN Microsystems' work stations is available from the authors on request.
[25]P. S. Lomdahl, O. H. Olsen, and M. R. Samuelsen, Phys. Rev. A **29**, 350 (1984).
[26]D. W. McLaughlin and A. C. Scott, Phys. Rev. A **18**, 1652 (1978).

[27]R. E. Glover and H. T. Coffey, Rev. Mod. Phys. **36**, 299 (1964).

[28]N. P. Ong, K. Verma and K. Maki, Phys. Rev. Lett. **52**, 663 (1984).

[29]G. Verma and N. P. Ong, Phys. Rev. B **30**, 2928 (1984).

[30]L. P. Gor'kov, Pis'ma Zh. Eksp. Teor. Fiz. **38**, 76 (1983) [Sov. Phys.—JETP Lett. **38**, 87 (1983)]; I. Batistić, A. Bjelis, and L. P. Gorkov, J. Phys. **45**, 1049 (1984).

[31]D. S. Fisher, Phys. Rev. B **31**, 1396 (1985).

[32]G. Travaglini and P. Wachter, Lect. Notes Phys. **217**, 115 (1985).

[33]R. M. Fleming, D. E. Moncton, and D. B. McWhan, Phys. Rev. B **18**, 5560 (1978).

[34]B. Horovitz and S. E. Trullinger, Solid State Commun. **49**, 195 (1984).

[35]S. Barišić and I. Batistić, J. Phys. Lett. **46**, L819 (1985).

[36]P. Monceau, M. Renard, J. Richard, M. C. Saint-Lager, H. Salva, and Z. Z. Wang, Phys. Rev. B **28**, 1646 (1983).

[37]A. T. Fiory, Phys. Rev. Lett. **27**, 501 (1971).

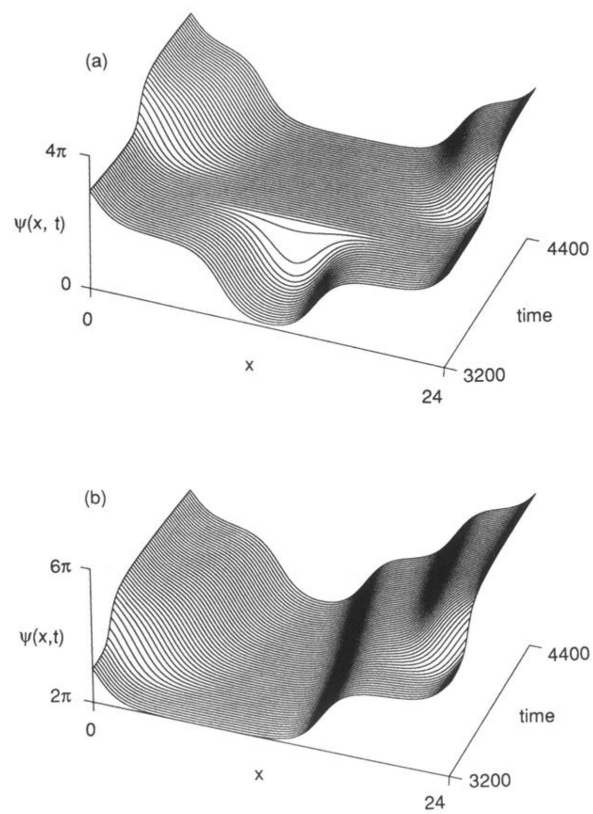

FIG. 6. Time evolution of $\psi(x,t)$ with inhomogeneous field $\Gamma_0=0.02$, $A=4.17$ [Eq. (5)], $\epsilon=10$, and (a) $n_k=0$, (b) $n_k=\frac{1}{24}$.